J. Fluid Mech. (1969), *vol.* 39, *part* 4, *pp.* 667–694
Printed in Great Britain

The radiatively driven discrete acoustic wave

By A. C. COGLEY†
Department of Aeronautics and Astronautics, Stanford University

(Received 19 December 1968 and in revised form 26 June 1969)

A complete and detailed study of a radiatively driven plane acoustic wave in a non-grey radiating and absorbing gas is carried out on the assumption of local molecular equilibrium. Specifically, the response of the gas in a semi-infinite space to a step input of radiation from a stationary black wall is investigated. The problem is physically interesting because radiative heat addition is the only driving mechanism, and this mechanism is unique and fundamental to the field of radiative gas dynamics. The solution shows that the heat addition gives rise initially to a compression-expansion wave in the gas, with the wave front controlled by radiation. This wave-front disturbance, though caused initially by the direct effect of radiative transfer, eventually outruns the region of appreciable heating near the wall and becomes a modified-classical disturbance that propagates away from the wall at the isentropic speed of sound. The radiative heat addition continues directly to affect the gas near the wall and in this manner drives the modified-classical wave indirectly by causing the formation of an 'effective gas piston'. The solution thus exhibits a linearized phenomenology corresponding to that observed in the non-linear leading wave associated with the nuclear fireball.

1. Introduction

We study here the problem of a radiatively driven plane acoustic wave in a non-grey radiating and absorbing gas. We investigate in particular the response of the gas in a semi-infinite half-space to a step change in temperature of a stationary black wall. The problem is physically interesting because radiative heat addition, which is the only driving force in the problem, has no counterpart in classical acoustic theory. We study only the linearized problem, since our main concern is for an intuitive understanding of how radiation by itself can supply the driving mechanism for gas-dynamic effects. The results, however, provide a basic first step toward understanding the corresponding non-linear phenomena. The work is part of a theoretical and experimental study of radiatively driven wave phenomena under way at Stanford University (cf. Long & Vincenti 1967).

Mathematically, this paper is a companion to Cogley & Vincenti (1969) (the paper immediately preceding). A familiarity with that paper will be presumed,

† Present address: Department of Energy Engineering, University of Illinois, Chigago.

and is essential for a detailed understanding of how the solution is obtained. It will become apparent that the method of Whitham (1959), as extended to radiative acoustics in the preceding paper, permits us to obtain an approximate analytical solution, where various other mathematical techniques would most likely have failed. As for the mechanically driven wave of the preceding paper, the two contributions that are needed to make up the solution are not of the same order of magnitude at all times. They are always equally important, however, in constructing the physically correct response. The approximate method again allows us to handle these two contributions in a successful manner, where more conventional mathematical methods would usually pick up only the contribution of larger magnitude.

The existing literature contains one paper directly related to our problem. Baldwin (1962) discussed, in an appendix, a formulation of the problem and presented an approximate solution for the temperature wave form by a different, more conventional method. He did not attempt a general solution for all dependent variables, and his temperature wave form did not include certain of the important physical phenomena that are evidenced here.

A paper indirectly related to our problem is that of Solan & Cohen (1966). This was part of a series in which the Rayleigh problem for a radiating compressible gas was investigated (cf. Solan & Cohen 1967*a*, *b*). The general formulation of these authors is for a grey gas and includes, of course, viscosity and thermal conduction. In the simplifications of the 1966 paper, where the Boltzmann number (the ratio of wave energy flux to radiant energy flux) is assumed large and the time small, the viscous and conduction effects become negligible in the outer flow. The governing equation also becomes linear, and the resulting physical problem is closely related to the present one. That is, the horizontally moving plate is convectively heated by viscous effects in a boundary layer of negligible thickness, and the heated plate then radiatively induces a response outside the layer. Other minor differences also exist between the two problems. The present solution is similar to Solan & Cohen's, however, within the limited time region in which their results are valid.

The mathematics of the present problem is similar to that of the mechanically driven wave of the preceding paper, in that the governing differential equations and the general approach to the approximate solution are identical. The only difference is in the driving disturbance. Thus, everything said about the exact governing equation and the equivalent lower-order equations in the preceding paper applies equally well here. Also, as in the preceding paper, the present treatment is general in the sense that it applies over the entire range of non-grey Boltzmann numbers and for all values of the absorption coefficient. It is approximate in that it is restricted to certain small-, intermediate-, and large-time regions.

2. Formulation

The exact statement of the problem and its formal solution are set down in § 5 of the preceding paper. The solution is given by (1.32), and the c's and C's that

appear therein are determined by (1.29) and (1.30, 1.31), respectively.† For the present problem of a stationary wall, we take $u_w = 0$ in the latter equations. Again, since c_I, c_{II}, C_I and C_{II} are such complicated functions of the transform variable s, a complete investigation of the exact solution would involve prohibitive labour, and an exact closed-form solution may even be impossible. An approximate solution is therefore again sought on the basis of the lower-order differential equations supplied by Whitham's method, as discussed in the preceding paper.

The Laplace transform of the solution based on these approximate equations is given by (1.37), where the various c's, together with their ranges of validity in s for various Bo_N, are given by (1.33)–(1.36). The term with c_S or c_T in (1.37), upon inversion, is the superposition of the modified-classical harmonic waves; the term with c_∞ or c_0, of the radiation-induced waves. The values of C_I and C_{II} again follow from (1.30, 1.31) with c_I replaced by c_S or c_T and c_{II} by c_∞ or c_0. As in the solution for the mechanically driven wave, the transformed solution (1.37) need not be inverted as it stands. Expansions compatible with the approximate method are carried out for the appropriate c's and the C's, and the resulting simplified solution is inverted. Appeal is then made to the Abelian theorems for the Laplace transform to interpret the inverted results (cf. Cogley & Vincenti 1969).

In §6 of the preceding paper we introduced the terminology of 'modified-classical' and 'radiation-induced' contributions to denote the results of superposing the modified-classical and radiation-induced harmonic waves, respectively. In the present problem this nomenclature becomes misleading, because the entire response is radiation-induced in the sense that radiation is the sole driving mechanism. We therefore adopt the terminology 'radiation-*controlled*' wave (or contribution) to denote the superposition of the radiation-induced harmonic waves. We shall see that this is physically meaningful, since this superposition always gives rise to that part of the discrete wave that is predominantly controlled by radiative transfer. The terminology 'modified-classical' wave (or contribution) is retained for the superposition of the modified-classical harmonic waves. This contribution always acts like a classical acoustic wave in a non-radiating gas, slightly modified by radiative transfer. The foregoing is, of course, a mathematical division of the problem, and the gas itself exhibits only the sum of the two contributions. When the contributions are of comparable magnitude in a region of the flow field, the nomenclature is not particularly helpful, because it does not then suggest the actual behaviour of the gas. Many situations arise, however, in which the contributions are not of comparable size in a given region. In such situations the name of the larger contribution conveys which physical process determines the wave and how the wave propagates in that region.

A diagram summarizing the phenomenology that will appear in the solution is given in figure 1. This diagram, which corresponds to figure 1.4, for the

† The prefix 1 will be used to denote equations and figures that appear in the preceding paper. All mathematical symbols are identical to those used previously, and therefore will not be defined here.

mechanically driven wave, shows the regions of validity of the approximate solution in the Bo_N, τ plane and gives the dimensionless groupings that govern the solution. The important physical phenomena are also indicated, but the detailed significance of the figure will become apparent only as the solution is obtained.

The solution by Whitham's method is carried out in §3 and §4. In §3 the solution for $Bo_N \gg 16\sqrt{\gamma_0}$ (weak radiation) is developed and discussed in detail. We then summarize in §4 the solution for $Bo_N = O(16\sqrt{\gamma_0})$ and $Bo_N \ll 16\sqrt{\gamma_0}$

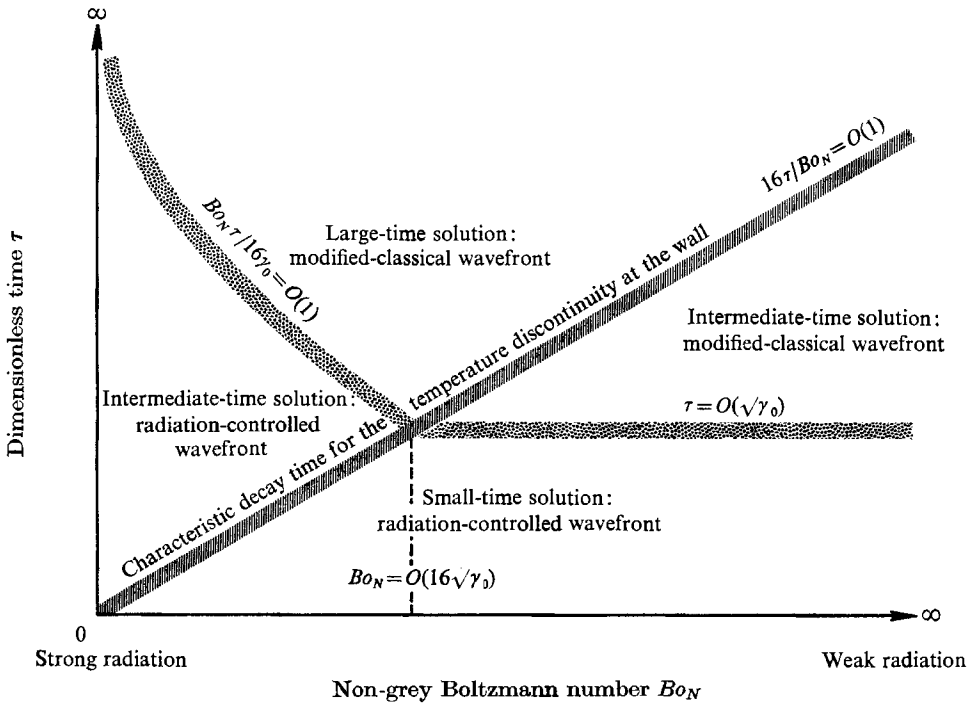

FIGURE 1. Schematic representation of solution for the radiatively driven plane wave. (Bo_N is defined in §3 of Cogley & Vincenti 1969.) ▦, transition from radiation-controlled wave front to modified-classical wave front; ▨, transition of the radiative heat addition from purely absorptive to diffusive.

(strong radiation), presenting only those details and results that are essential for an understanding of the complete solution. Little physical insight is lost by this abridgement, since the basic phenomenology of the solution is the same for all Bo_N. The details, however, do depend on Bo_N, so that at least some consideration of these matters is necessary.

In §5 a special limited solution, restricted by the requirement that $16\tau/Bo_N < 1$ (see figure 1), is obtained by a separate method. This solution supports the small- and intermediate-time portions of the weak-radiation solution of §3. For this range it supplies a solution that is continuously valid in τ, whereas the general approach leads to a somewhat troublesome transition region at $\tau = O(\sqrt{\gamma_0})$.

3. Solution for $Bo_N \gg 16\sqrt{\gamma_0}$ (weak radiation)

To obtain the solution in this range for small time, we expand the appropriate c's (1.33, 1.35) and the C's (1.30, 1.31) with $u_w = 0$ for large values of $|s|$. This leads to the following expressions:†

$$c_S = -s-g+O\left(\frac{g}{s^2}\right),$$

$$c_\infty = -1+O\left(\frac{8\gamma_0}{Bo_N s}\right),$$

$$C_I = \frac{8T_w}{Bo_N}\left(\frac{1}{s^4}+\frac{1}{\gamma_0 s^6}\right)+O\left(\frac{8T_w}{\gamma_0^2 Bo_N s^8}\right),$$

$$C_{II} = -\frac{8T_w}{Bo_N}\left(\frac{1}{s^3}+\frac{1}{\gamma_0 s^5}\right)+O\left(\frac{8T_w}{\gamma_0^2 Bo_N s^7}\right).$$

By putting these results into (1.37), the transformed potential function obtained is:

$$\bar{\phi}(\xi,s) = -\frac{8T_w}{Bo_N}\left(\frac{1}{s^3}+\frac{1}{\gamma_0 s^5}\right)\exp(-\xi)-\left(\frac{1}{s^4}+\frac{1}{\gamma_0 s^6}\right)\exp(-s\xi-g\xi). \tag{1}$$

Here the radiation-controlled terms are listed first on the right-hand side, because they usually represent the dominant contribution in the present problem. (This practice will be followed throughout.) As in the preceding paper, we are really interested in the physical variables, whose transforms are given in terms of $\bar{\phi}$ by the relations (1.38) through (1.41). Substituting from (1) into these relations, and inverting by means of tables (e.g. Erdélyi *et al.* 1954), we obtain the following results to $O(\tau^4)$:

$$\frac{u}{T_w} \cong \frac{8}{Bo_N}\left\{\left(\frac{\tau^2}{2!}+\frac{\tau^4}{\gamma_0 4!}\right)e^{-\xi}-\exp(-g\xi)\,S(\tau-\xi)\left[\frac{(\tau-\xi)^2}{2!}+\frac{1}{\gamma_0}\frac{(\tau-\xi)^4}{4!}\right]\right\}, \tag{2}$$

$$\frac{p}{T_w} \cong \frac{8\gamma_0}{Bo_N}\left\{\left(\tau+\frac{\tau^3}{\gamma_0 3!}\right)e^{-\xi}-\exp(-g\xi)\,S(\tau-\xi)\left[\frac{(\tau-\xi)^2}{2!}+\frac{1}{\gamma_0}\frac{(\tau-\xi)^4}{4!}\right]\right\}, \tag{3}$$

$$\frac{\rho}{T_w} \cong \frac{8}{Bo_N}\left\{\frac{\tau^3}{3!}e^{-\xi}-\exp(-g\xi)\,S(\tau-\xi)\left[\frac{(\tau-\xi)^2}{2!}+\frac{1}{\gamma_0}\frac{(\tau-\xi)^4}{4!}\right]\right\}, \tag{4}$$

$$\frac{T}{T_w} \cong \frac{8}{Bo_N}\left\{\gamma_0\tau e^{-\xi}-(\gamma_0-1)\exp(-g\xi)\,S(\tau-\xi)\left[\frac{(\tau-\xi)^2}{2!}+\frac{1}{\gamma_0}\frac{(\tau-\xi)^4}{4!}\right]\right\}, \tag{5}$$

where $S(\tau-\xi)$ is the unit step function. The terms with the step function are the modified-classical contribution; the remaining terms are the radiation-controlled contribution. Since this latter contribution attenuates as $e^{-\xi}$, the radiant heat transfer due to spontaneous emission from the gas is negligible compared with that due to the radiation from the wall (cf. Gilles, Cogley & Vincenti 1969, (25)), i.e. the heat addition takes place here by simple absorption. At larger times we will see that the gaseous radiation becomes important; radiative heat

† The parameter $g \equiv 8(\gamma_0-1)/Bo_N$ is again used for the reasons given in Cogley & Vincenti (1969, §6).

addition and transport will then become diffusive. The above solution gives no discontinuities in the physical variables themselves, but the step function does cause certain of their second derivatives to be discontinuous at $\xi = \tau$. This solution is valid for dimensionless times up to $O(\sqrt{\gamma_0})$.

We see that the velocity at the wall ($\xi = 0$) is zero as required by the boundary condition, and the corresponding temperature and pressure disturbances increase, to first order, linearly with time. The perturbation density is negative for small values of ξ, becomes positive at larger distances, and then goes to zero for very large ξ. Numerical results from this small-time solution for $Bo_N = 2 \times 10^3$ and $\gamma_0 = 1{\cdot}4$ are shown in figures 2, 3 and 4. These are three-dimensional plots of

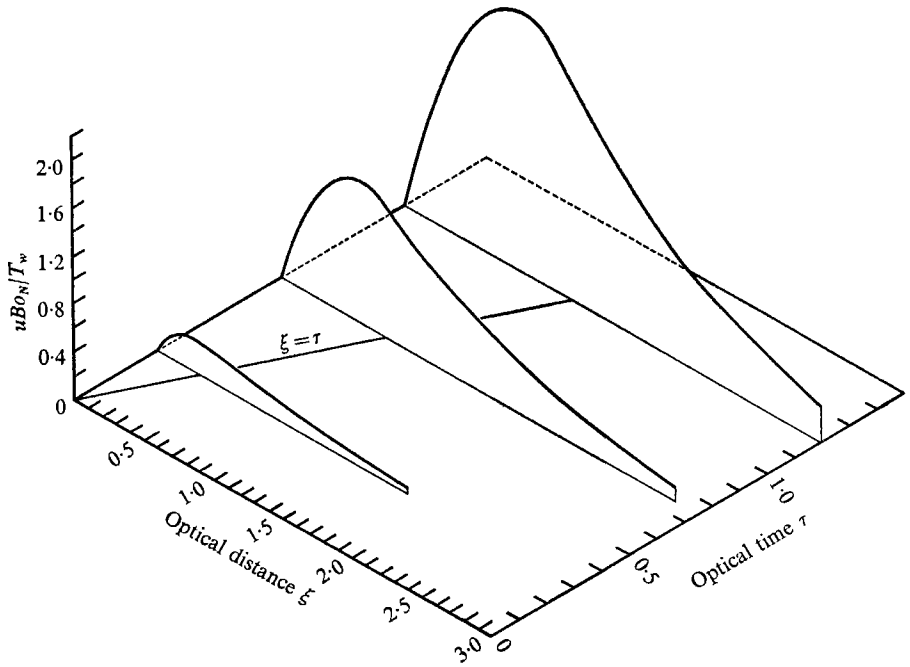

FIGURE 2. Velocity response for small time, $\gamma_0 = 1{\cdot}4$, $Bo_N = 2 \times 10^3$.

the normalized dependent variables *versus* the optical distance ξ and what we refer to as the optical time τ. (For definition of the normalized physical variables, see Cogley & Vincenti 1969, §3.) The optical distance $\xi \equiv n_0 x$ is obtained by normalizing the physical distance by a non-grey radiative mean free path $1/n_0$ (where n_0 represents an effective frequency-averaged absorption coefficient; see Gilles, Cogley & Vincenti 1969). Time is normalized by the time it would take a classical isentropic acoustic wave to travel one radiative mean free path, i.e. $\tau \equiv n_0 a_{S_0} t$. The line $\xi = \tau$ on these plots thus shows where an isentropic acoustic disturbance would have propagated starting from the wall at time zero.

Figures 2 and 3 for the velocity and density, respectively, show a compression-expansion wave propagating into the gas. The strength of this wave increases with time as a result of the radiant heat transfer from the wall. The normalized temperature and pressure disturbances in figure 4 are almost equal for very small

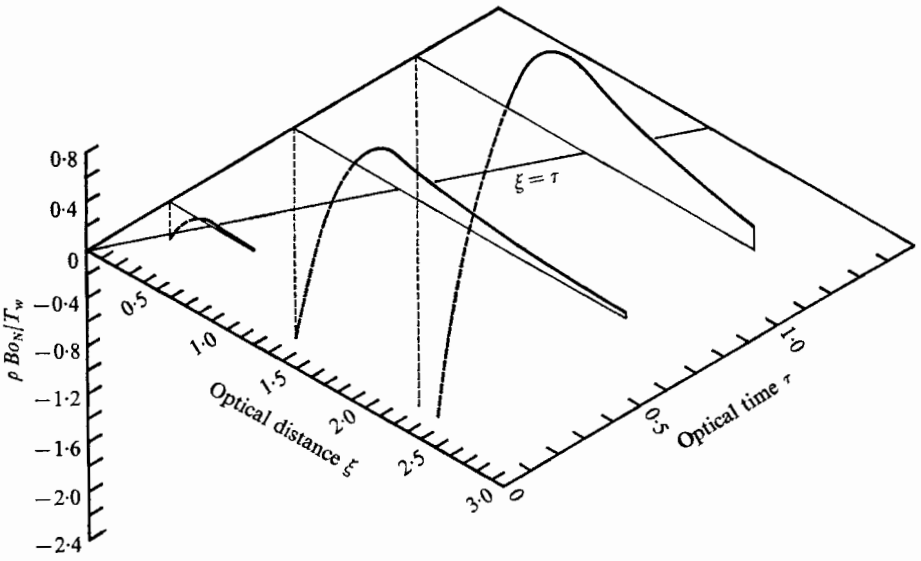

FIGURE 3. Density response for small time, $\gamma_0 = 1{\cdot}4$, $Bo_N = 2 \times 10^3$.

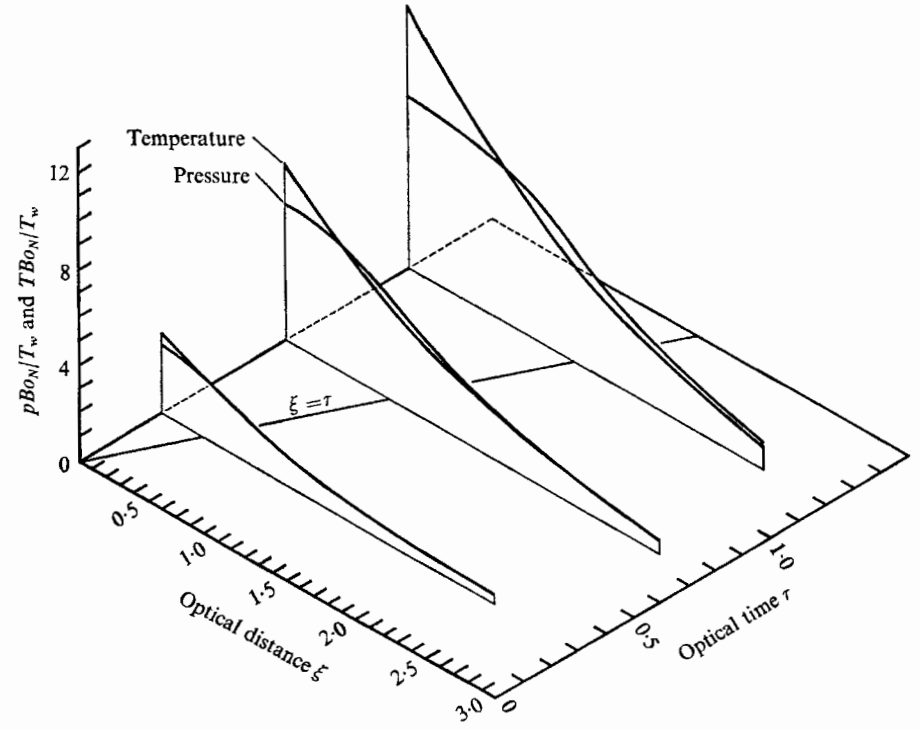

FIGURE 4. Temperature and pressure response for small time, $\gamma_0 = 1{\cdot}4$, $Bo_N = 2 \times 10^3$.

time. As time increases, however, the pressure falls below the temperature at small ξ and rises above it at larger ξ. This type of response is caused by the inertia of the gas, i.e. the temperature and pressure must respond initially in much the same manner (as required by the equation of state), since the heat transfer acting through the pressure gradient has not had time to set the gas in motion and significantly alter its density. At later times the inertia of the gas is overcome, the density changes appreciably, and the pressure need no longer follow the temperature. The excess of pressure over temperature at the larger times and

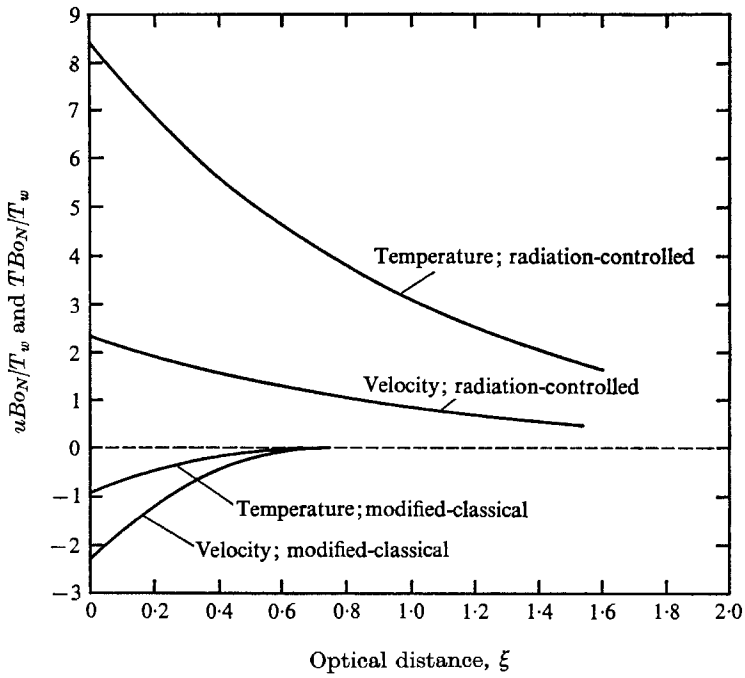

FIGURE 5. Modified-classical and radiation-controlled contributions to the total wave form, $\gamma_0 = 1{\cdot}4$, $Bo_N = 2 \times 10^3$, $\tau = 0{\cdot}75$.

distances in figure 4 is essential, because the disturbance produced by the non-uniform heating must eventually propagate away from the wall as a modified-classical wave. For this to occur, the ratio p/T must ultimately approach the classical value of $\gamma_0/(\gamma_0 - 1)$ near the front of the wave (near $\xi = \tau$). We shall see this transition to a modified-classical wave front become complete in the next time region.

It should be noted that in the small-time region the radiation-controlled contribution to the discrete wave is felt ahead of the modified-classical contribution. This is shown in figure 5, where the separate contributions are presented for temperature and velocity at $\tau = 0{\cdot}75$. The radiation-controlled contribution is dominant for these small times except near the wall ($\xi < \tau$), where the modified-classical contribution acts as a boundary layer to the total response.

As in the discussion of the mechanically driven wave in the preceding paper, the mathematical structure of c_0 in (1.35), which also affects C_I and C_{II}, dictates

an intermediate-time solution when $Bo_N \gg 16\sqrt{\gamma_0}$. This time corresponds through the Abelian theorems to expansions of the appropriate c's and the C's for small but finite $|s|$ in the annular region $16/Bo_N < |s| < 1$. The results are:

$$c_S = -s + gs^2 + O(gs^4),$$

$$c_0 = -1 + O\left(\frac{8}{Bo_N s}\right),$$

$$C_I = -\frac{8T_w}{Bo_N s^2} + O\left(\frac{T_w}{s}\left(\frac{8}{Bo_N s}\right)^2\right),$$

$$C_{II} = \frac{8T_w}{Bo_N s} + O\left(T_w\left(\frac{8}{Bo_N s}\right)^2\right).$$

Using these expressions, we find that the transformed dependent variables are:

$$\frac{\bar{u}}{T_w} \cong \frac{8}{Bo_N}\left\{-\frac{1}{s}e^{-\xi} - \frac{1}{s^2}(-s+gs^2)\exp\left[(-s+gs^2)\xi\right]\right\}, \tag{6}$$

$$\frac{\bar{p}}{T_w} \cong \frac{8\gamma_0}{Bo_N}\left\{-e^{-\xi} + \frac{1}{s}\exp\left[(-s+gs^2)\xi\right]\right\}, \tag{7}$$

$$\frac{\bar{\rho}}{T_w} \cong \frac{8}{Bo_N}\left\{-\frac{1}{s^2}e^{-\xi} + \frac{1}{s^3}(-s+gs^2)^2\exp\left[(-s+gs^2)\xi\right]\right\}, \tag{8}$$

and

$$\bar{T} = \bar{p} - \bar{\rho}. \tag{9}$$

The terms giving the radiation-controlled contribution in these equations can be inverted by means of tables. The modified-classical contribution can be inverted by the method of steepest descent. If the higher-order modified-classical terms in (6) and (8) are dropped, the inversion integral needed is

$$I = \frac{1}{2\pi i}\int_\Gamma \frac{1}{s}\exp\{s\tau - s\xi + gs^2\xi\}\,ds.$$

This integral has been evaluated by Cogley (1968) for the appropriate Bromwich path; the result is

$$I \cong \left\{1 - \frac{1}{2}\operatorname{erfc}\left[\frac{(\tau-\xi)}{2\sqrt{g\xi}}\right]\right\}, \tag{10}$$

which is the same type of result obtained in Cogley & Vincenti (1969, §6). Dropping the higher-order terms leads to considerable simplification in the solution with no real loss in physical meaning of the results; we merely lose sight of the fact that the dependent variables are not all diffused in precisely the same manner in the modified-classical contribution to the wave. The simplified solution obeys the classical acoustic relationships,

$$p_{mc} = \gamma_0 u_{mc}, \quad \rho_{mc} = u_{mc}, \quad \text{and} \quad T_{mc} = (\gamma_0 - 1)u_{mc}, \tag{11}$$

which will hold for the isentropic modified-classical (mc) contribution throughout

this work. The intermediate-time solution, correct to $O(16\tau/Bo_N)$, is thus written finally as

$$\frac{u}{T_w} \simeq \frac{8}{Bo_N}\{e^{-\xi} + I\}, \tag{12}$$

$$\frac{p}{T_w} \simeq \frac{8\gamma_0}{Bo_N} I, \tag{13}$$

$$\frac{\rho}{T_w} \simeq \frac{8}{Bo_N}\{-\tau e^{-\xi} + I\}, \tag{14}$$

$$\frac{T}{T_w} \simeq \frac{8}{Bo_N}\{\tau e^{-\xi} + (\gamma_0 - 1) I\}, \tag{15}$$

where the radiation-controlled term in (7) has inverted to a non-contributing delta function.

These results are valid in the region $\sqrt{\gamma_0} < \tau < Bo_N/16$ (see figure 1) except in one respect. In obtaining the results, we have expanded the two terms that appear in the transformed solution (1.37) and inverted them separately. It is shown by Cogley (1968), however, that these two separate terms, as well as their exact counterparts, are not individually analytic in the right-hand side of the complex s-plane. Only the sum of the two terms represents an analytic function in this region. The problem here is associated with the branch points of the exact formulation, and with our inability to follow a given contribution across certain transition regions, both of which matters are discussed later. Our procedures in the present region are therefore not completely valid, and this results in a loss of information about how the wave form was started at the smaller times. This leads to a quantitative inaccuracy at the wave front ($\xi = \tau$) in the above results. This is not really a difficulty, however, because an independent limited solution can be obtained that is continuously valid over the small- and intermediate-time regions. This solution is given in § 5, and its results can be used to supplement the present results at the wave front. The present solution is presented because its separation of the problem into radiation-controlled and modified-classical contributions leads to important physical insight. Away from the wave front the results from the two approaches coincide within a few per cent.

A plot of the two contributions to velocity and temperature for $Bo_N = 2 \times 10^3$ is given in figure 6 for a representative time in the intermediate-time region. In a reversal of the roles observed at small time (figure 5), the modified-classical contribution is now felt ahead of the radiation-controlled contribution, which now provides the boundary layer. Near the wave front ($\xi = \tau$), the modified-classical contribution dominates, and the discrete isentropic front acts almost like a purely gas-dynamic disturbance, i.e. for all practical purposes the modified-classical disturbances are related by $T_{mc} = (\gamma_0 - 1)u_{mc}$, for the reasons discussed prior to (11). This is true in both approaches to the solution, and thus the limited solution of § 5 substantiates our dropping the higher-order terms in the present solution (cf. discussion prior to (11)). In the vicinity of the wave front, the broken line represents the results from the present solution, while the solid line is the more exact solution from § 5. In all following plots for intermediate time, only this more exact wave front will be shown.

Comparing figures 5 and 6, we see that the two mathematically separate contributions (modified-classical and radiation-controlled) do not retain a continuous identity through the transition region between the small- and intermediate-time regions. The following figures will show, however, that the total or physical wave form is continuous. The lack of continuity of the individual contributions is disconcerting at first, since one naturally wants to follow, say, the modified-classical contribution from one time region to the next as a physical entity that affects the gas. This cannot be done in general, because across certain transition regions the radiation-controlled contribution in fact turns into the modified-classical contribution and vice versa. The mathematical reason for this is discussed by Cogley (1968), and concerns the branch points of the exact problem.

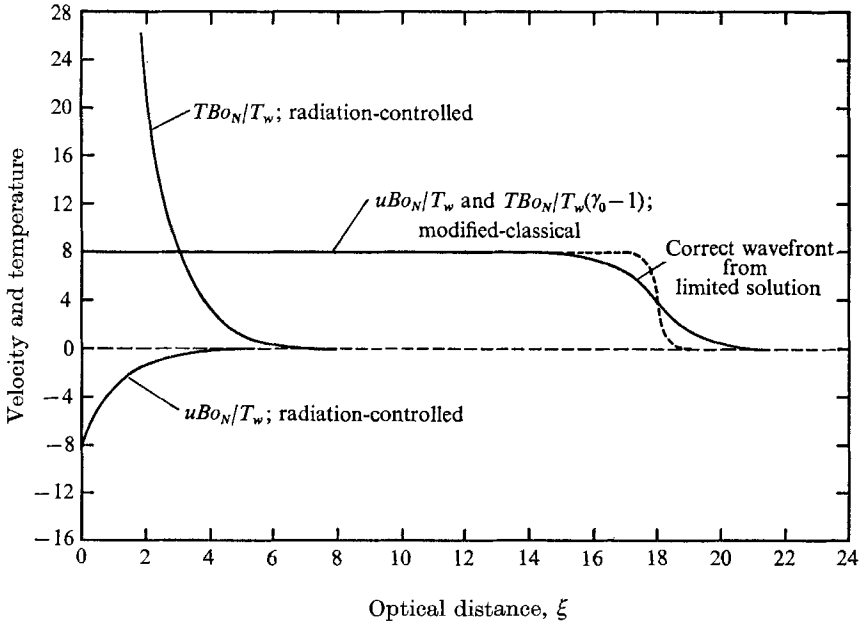

FIGURE 6. Modified-classical and radiation-controlled contributions to the total wave form, $\gamma_0 = 1{\cdot}4$, $Bo_N = 2 \times 10^3$, $\tau = 18{\cdot}0$.

The present splitting of the solution is only mathematical and approximate and has physical meaning only when the gas response is identifiable primarily with one contribution in a given space-time region. Within certain transition regions the response is of one piece, and the division into modified-classical and radiation-controlled contributions is not possible.

Three-dimensional plots of the wave forms for the intermediate-time region are given in figures 7 through 9. The velocity and density response of figures 7 and 8 show the continuation of the compression-expansion wave set up in the small-time region. The compressive part of the wave (the wave front near $\xi = \tau$), now given by the modified-classical contribution, is the physical extension of the radiation-controlled contribution from the small-time region. That is, the disturbance created at small time by radiant heat addition has now outrun the

immediate effects of the wall radiation, and is propagating away from the wall as a discrete modified-classical wave at the isentropic speed of sound. This modified-classical wave front diffuses only slightly in this time region, since the gas itself is only weakly radiating. Near the wall (i.e. within a few radiative mean free paths) the radiation-controlled contribution now provides the expansion part of the wave, still through simple absorption of the radiation from the wall. The overall picture in this time region is thus clear: Radiant heating of a layer of gas near the wall causes the gas to expand, and this expanding layer acts as an effective piston driving an essentially classical wave of almost uniform magnitude. This concept of an effective gas piston will be useful later.

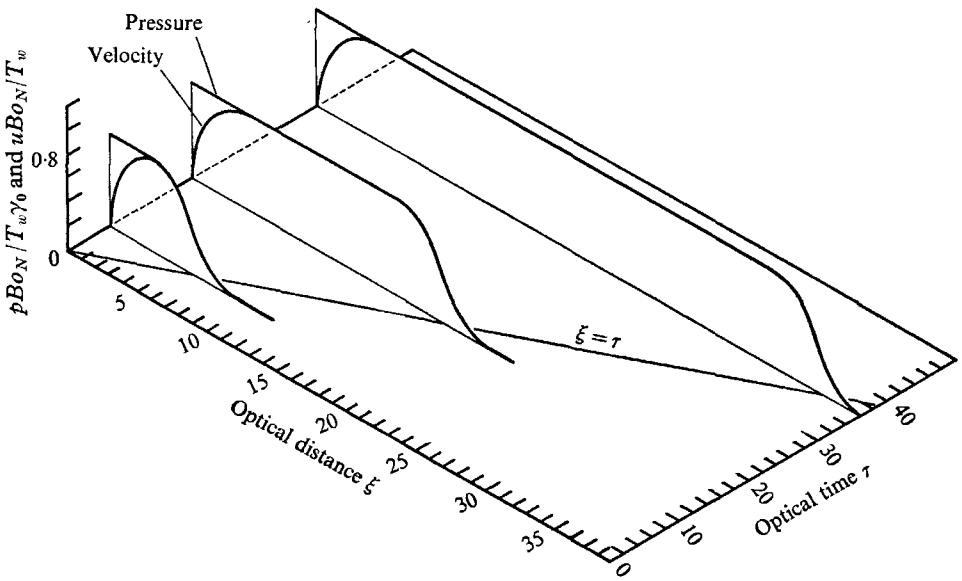

FIGURE 7. Velocity and pressure response for intermediate time, $\gamma_0 = 1{\cdot}4$, $Bo_N = 2 \times 10^3$.

The pressure is plotted in figure 7 as $pBo_N/T_w\gamma_0$ to emphasize that the major portion of the wave conforms closely to the classical relationship $p = \gamma_0 u$. Only near the wall, where the radiation is felt directly, does this pressure parameter deviate from the velocity.

It should be noted that figure 8 is plotted on two different vertical scales, and the scale for ξ is broken to bring both phenomena of interest into view. Since the break is made where the density is nearly uniform, no essential information is lost. The magnitude of the density disturbance in the wave front is seen to be small relative to that near the wall. This is so because the part of the wave that is more than a few radiative mean free paths from the wall receives little radiant energy directly. It is driven only indirectly through the action of the expanding gas piston.

The temperature is plotted in figure 9 in much the same manner as the density. The gas is heated rapidly next to the wall by direct radiant heat transfer, and this energy input drives, again through the gas piston, a relatively small

temperature 'precursor' in the form of an essentially classical discrete wave (cf. figures 7 and 8). From (15) we see that the temperature discontinuity between the wall and the gas immediately adjacent to it decreases linearly with time, and

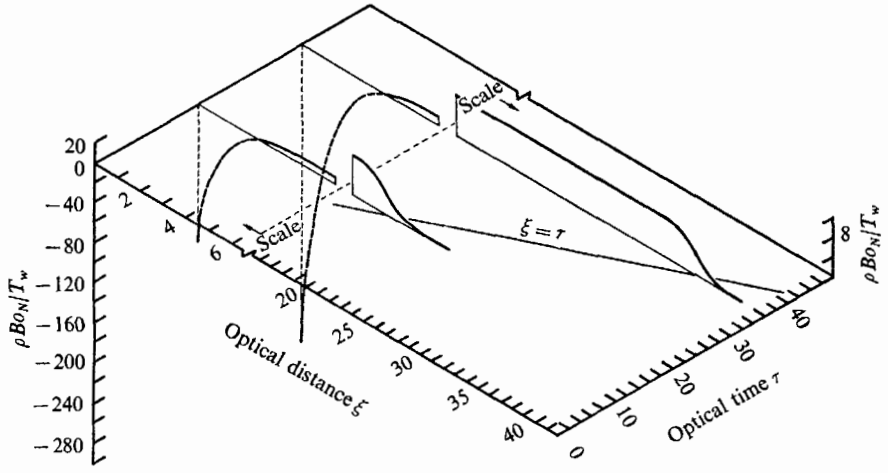

FIGURE 8. Density response for intermediate time, $\gamma_0 = 1{\cdot}4$, $Bo_N = 2 \times 10^3$.

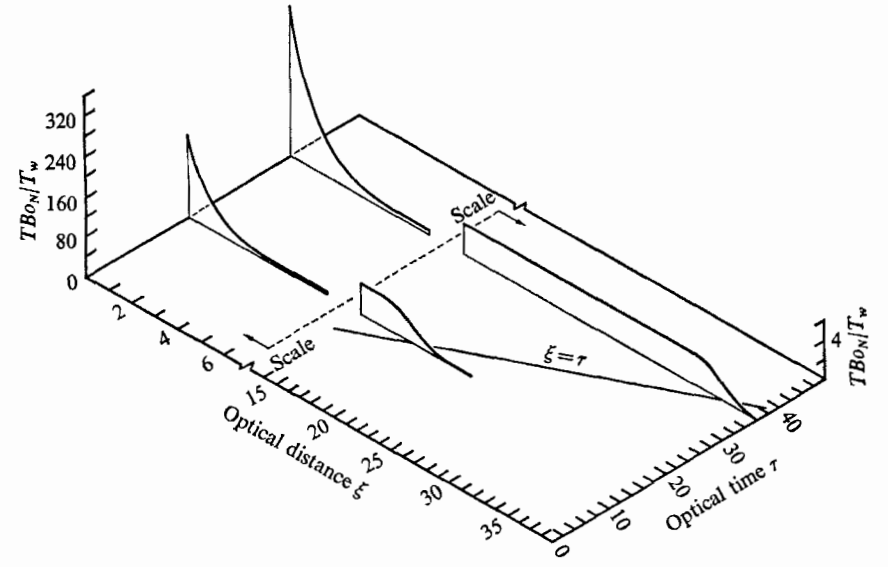

FIGURE 9. Temperature response for intermediate time, $\gamma_0 = 1{\cdot}4$, $Bo_N = 2 \times 10^3$.

will essentially disappear (i.e. $T(\xi = 0) = T_w$) at the end of the intermediate-time region (see figure 1).†

In the limit as $Bo_N \to \infty$, the small- and intermediate-time solutions make up the total solution (see figure 1). In this limit all perturbations given by both

† Baldwin (1962) has shown that the temperature discontinuity actually decays exponentially. We have merely picked up the linear terms as the result of our expansions. Our characteristic decay time, however, is equivalent to his.

solutions go to zero, representing no response. This is the same result that one would obtain from the exact governing equation (1.6) by first taking the limit $Bo_N \to \infty$ and then solving the remaining trivial problem. This is, of course, the physically correct result. When $Bo_N \to \infty$, the gas neither emits nor absorbs radiation, which is the only driving force present in the problem. The response is therefore zero throughout.

To complete our story for $Bo_N \gg 16\sqrt{\gamma_0}$, the large-time solution is found by again expanding the appropriate c's and the C's for small $|s|$, specifically for $|s| < 16/Bo_N$. This results in:

$$c_S = -s + gs^2 + O(gs^4),$$

$$c_0 = -\left(\frac{sBo_N}{16}\right)^{\frac{1}{2}} + O\left(\left(\frac{sBo_N}{16}\right)^{\frac{3}{2}}\right),$$

$$C_I = -T_w\left\{\left(\frac{16}{sBo_N}\right)^{\frac{1}{2}}\frac{1}{s}\right\} + O(T_w/s),$$

$$C_{II} = T_w\left\{\frac{16}{sBo_N} - \left(\frac{16}{sBo_N}\right)^{\frac{1}{2}}\right\} + O(T_w).$$

The transformed dependent variables follow as

$$\frac{\bar{u}}{T_w} \cong \left(1 - \left(\frac{16}{sBo_N}\right)^{\frac{1}{2}}\right)\exp\left(-\left(\frac{sBo_N}{16}\xi\right)^{\frac{1}{2}}\right) + \left(\frac{16}{sBo_N}\right)^{\frac{1}{2}}\exp(-s\xi + gs^2\xi), \tag{16}$$

$$\frac{\bar{p}}{T_w} \cong \gamma_0\left\{\left(\left(\frac{16s}{Bo_N}\right)^{\frac{1}{2}} - \frac{16}{Bo_N}\right)\exp\left(-\left(\frac{sBo_N}{16}\xi\right)^{\frac{1}{2}}\right) + \left(\frac{16}{sBo_N}\right)^{\frac{1}{2}}\exp(-s\xi + gs^2\xi)\right\}, \tag{17}$$

$$\frac{\bar{\rho}}{T_w} \cong \left(\left(\frac{Bo_N}{16s}\right)^{\frac{1}{2}} - \frac{1}{s}\right)\exp\left(-\left(\frac{sBo_N}{16}\xi\right)^{\frac{1}{2}}\right) + \left(\frac{16}{sBo_N}\right)^{\frac{1}{2}}\exp(-s\xi + gs^2\xi), \tag{18}$$

and temperature is merely the difference between pressure and density as in (9). The radiation-controlled terms in these equations can again be inverted by means of tables, with results valid for all ξ. The modified-classical terms could be inverted by the method of steepest descent and, as they stand, would lead to the correct contribution away from the wave front (i.e. away from $\xi = \tau$). In expanding $C_I c_S$, which is the function that represents the speed of the effective gas piston, for large time, however, we have lost information about the speed at intermediate times that is essential if we wish to obtain the correct wave form in the vicinity of the wave front itself.† In contrast to the situation at intermediate time, the loss of information here is not connected with the branch points or the resulting inability to follow a given contribution across the transition region; the modified-classical contribution is, in fact, a physically continuous wave across the region $16\tau/Bo_N = O(1)$. The present problem did not arise in the mechanically driven wave, because the speed of the mechanical piston was constant for all $\tau > 0$.

The needed information can be picked up by working from a more general expression for the speed of the effective piston $C_I c_S = -C_{II} c_0$, which drives the

† An unrealistic infinite response is obtained at the wave front without this modification.

modified-classical velocity contribution (cf. (1.30) with $u_w = 0$). We proceed as follows: The more general expression is

$$\bar{u}(0,s)_{mc} = C_I c_S = -C_{II} c_0 = -T_w \frac{(c_0+1)}{c_0} + O\left(T_w \frac{16s}{Bo_N}\right). \tag{19}$$

We now use the complete expression (1.36) for c_0, rather than its expansion for $|s| < 16/Bo_N$, to obtain

$$\left.\frac{\bar{u}(0,s)}{T_w}\right|_{mc} \cong \left(\frac{s+16/Bo_N}{s}\right)^{\frac{1}{2}} - 1. \tag{20}$$

This result can be inverted by means of tables to give

$$\left.\frac{u(0,\tau)}{T_w}\right|_{mc} \cong \frac{8}{Bo_N} \exp(-8\tau/Bo_N)\{I_1(8\tau/Bo_N) + I_0(8\tau/Bo_N)\}, \tag{21}$$

where I_1 and I_0 are modified Bessel functions of the first kind. Equation (21) provides an expression for the speed of the effective gas piston that is continuously valid in the intermediate- and large-time regions. We can verify this by first expanding (21) for $16\tau/Bo_N < 1$. This gives

$$\left.\frac{u(0,\tau)}{T_w}\right|_{mc} \cong \frac{8}{Bo_N} + \ldots,$$

which is precisely the modified-classical term in the intermediate-time solution of (12) evaluated at $\xi = 0$. This represents a constant speed for the effective gas piston that was observed for intermediate times. Expanding (21) alternatively for $16\tau/Bo_N > 1$, we obtain

$$\left.\frac{u(0,\tau)}{T_w}\right|_{mc} \cong \left(\frac{16}{\tau Bo_N \pi}\right) + \ldots, \tag{22}$$

which is the same as one finds by inverting the leading-order modified-classical term in the large-time result (16) at $\xi = 0$. This shows that the speed of the effective gas piston slows up at large time like $1/\sqrt{\tau}$.

A valid expression for all ξ for the modified-classical contribution to the transformed velocity in (16) can now be obtained by replacing the coefficient of the second exponential term by the expression (20). We thus obtain, for all ξ at large time,

$$\left.\frac{\bar{u}(\xi,s)}{T_w}\right|_{mc} \cong \left\{\left(\frac{s+16/Bo_N}{s}\right)^{\frac{1}{2}} - 1\right\} \exp(-s\xi + gs^2\xi). \tag{23}$$

This result can be inverted by a combination of the method of steepest descent and convolution to give (cf. Cogley 1968):

$$\left.\frac{u(\xi,\tau)}{T_w}\right|_{mc} \cong \left(\frac{1}{4g\pi\xi}\right)^{\frac{1}{2}} \int_0^\tau \left\{\frac{8}{Bo_N} \exp(-8(\tau-\tilde{\tau})/Bo_N)\left[I_1\left[\frac{8}{Bo_N}(\tau-\tilde{\tau})\right] + I_0\left[\frac{8}{Bo_N}(\tau-\tilde{\tau})\right]\right]\right\} \exp\left(-\frac{(\tilde{\tau}-\xi)^2}{4g\xi}\right) d\tilde{\tau}. \tag{24}$$

Even though this result looks rather formidable, its physical meaning is not difficult to understand. Briefly, the integral tells us how the velocity input at $\tau - \tilde{\tau}$ (the term in braces, cf. (21)), which would be propagated invariantly in

classical acoustics, is changed by the diffusion due to radiant transfer within the gas. This diffusion is represented by the exponential function $\exp[-(\tilde{\tau}-\xi)^2/4g\xi]$, where the factor $4g$ is the diffusion coefficient.

The complete solution for large time can now be obtained in the physical variables by using tables to invert the radiation-controlled terms in (16)–(18) and then adding the modified-classical contribution as given by (24) and (11). The results correct to $O(\sqrt{Bo_N}/16\tau)$ are:

$$\frac{u}{T_w} \cong -\left(\frac{16}{\tau Bo_N \pi}\right)^{\frac{1}{2}} \exp\left(-\frac{\xi^2 Bo_N}{4(16)\tau}\right)\left\{1-\frac{Bo_N}{32}\frac{\xi}{\tau}\right\}+\left.\frac{u}{T_w}\right|_{mc}, \tag{25}$$

$$\frac{p}{T_w} \cong -\frac{\gamma_0}{2}\left(\frac{16}{Bo_N \pi}\right)^{\frac{1}{2}}\frac{\xi}{\tau^{\frac{3}{2}}}\exp\left(-\frac{\xi^2 Bo_N}{4(16)\tau}\right)\left\{1+\frac{1}{\xi}-\frac{Bo_N}{32}\frac{\xi}{\tau}\right\}+\left.\frac{\gamma_0 u}{T_w}\right|_{mc}, \tag{26}$$

$$\frac{\rho}{T_w} \cong -\left\{\operatorname{erfc}\left(\frac{\xi}{2}\left(\frac{Bo_N}{16}\right)^{\frac{1}{2}}\right)-\left(\frac{Bo_N}{16\tau\pi}\right)^{\frac{1}{2}}\exp\left(-\frac{\xi^2 Bo_N}{4(16)\tau}\right)\right\}+\left.\frac{u}{T_w}\right|_{mc}, \tag{27}$$

and $T = p-\rho$. It is evident in (25) that certain higher-order effects have been retained in the expression for $u(\xi,\tau)/T_w|_{mc}$, i.e. the condition of zero velocity at the boundary is not identically satisfied. This slight inconsistency is caused by our desire to obtain the correct wave form for all ξ. The velocity boundary condition is, however, satisfied to $O(\sqrt{Bo_N}/16\tau)$, which is all the accuracy claimed for the solution.

In this large-time region the density and temperature near the wall are governed by the complementary error function. Thus, the radiation from the wall has heated the gas near the wall to such an extent that the radiative heat addition is now a diffusive process. The small contributions to velocity and pressure from the radiation-controlled terms also reflect a diffusive process in that they decay like $\exp[-\xi^2 Bo_N/4(16)\tau]$. The rate of radiative energy input from the wall is now decreasing relative to what it was at intermediate times (because of the hot gas now adjacent to the wall), and the speed of the effective gas piston that drives the modified-classical part of the wave is hence slowing down like $1/\sqrt{\tau}$, as was seen in (22). Owing to this, and to the radiative heat transfer to the relatively cool surroundings, the small disturbance given by the modified-classical contribution dies off like $1/\sqrt{\tau}$ and spreads out like $\sqrt{\tau}$.

All these results for large time are apparent in figures 10, 11 and 12. In figures 11 and 12, broken horizontal scales and differing vertical scales are used as before; the line $\xi = \tau$ is also rotated as shown, so that the wave fronts can be presented. The velocity and density wave forms in figures 10 and 11 show the continuation and final form of the characteristic compression-expansion wave. The compressive part of the wave is mainly the modified-classical contribution, which propagates at the isentropic speed of sound. The expansive part is primarily the radiation-controlled contribution, which diffuses into the gas from the wall. The pressure parameter $pBo_N/T_w\gamma_0$ is plotted in figure 10 to emphasize the relationships in the portion of the wave dominated by the modified-classical contribution. As is apparent from figures 11 and 12, the density and temperature suffer their strongest effect within the radiation-controlled contribution near the wall. The density parameter increases monotonically from minus one at the wall to small positive

values at intermediate ξ, and then to larger positive values in the modified-classical wave front near $\xi = \tau$. The temperature parameter, as dictated by the equation of state, has a value of one at the wall and then decreases to small positive values for intermediate ξ. Ahead of this radiation-controlled temperature field is the small variation in temperature associated with the modified-classical contribution.

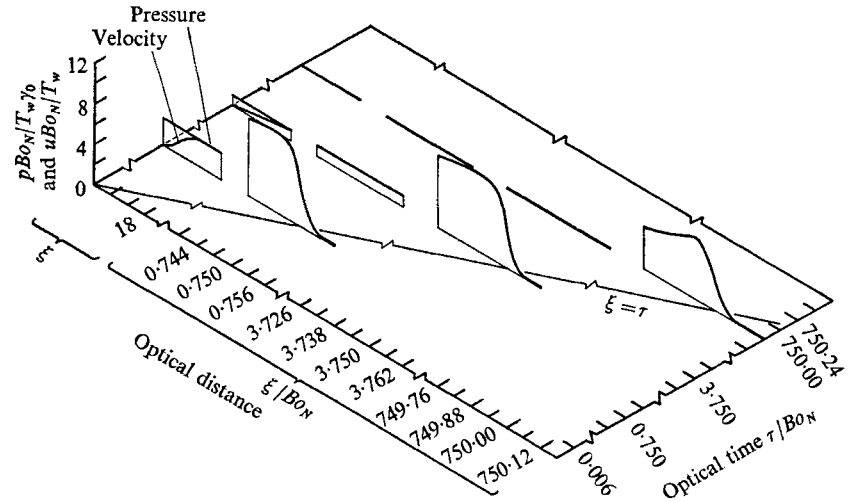

FIGURE 10. Velocity and pressure response for large time, $\gamma_0 = 1{\cdot}4$, $Bo_N = 2 \times 10^3$.

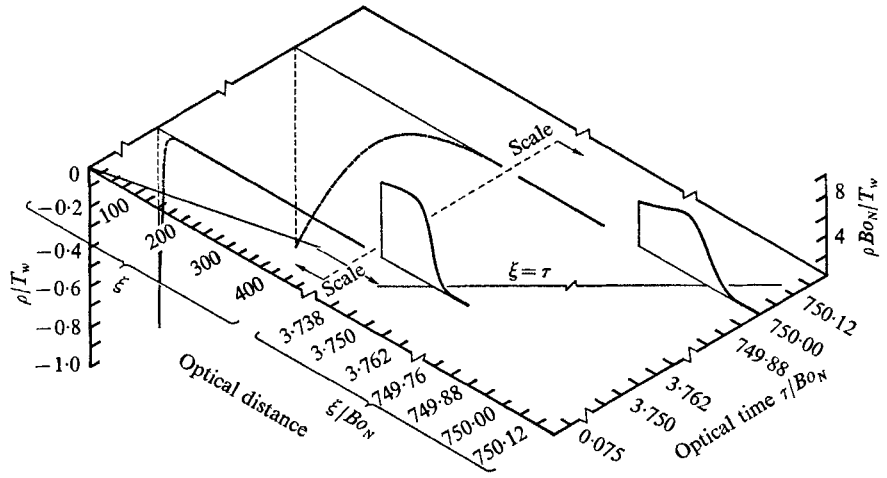

FIGURE 11. Density response for large time, $\gamma_0 = 1{\cdot}4$, $Bo_N = 2 \times 10^3$.

The overall phenomenology of the radiatively driven discrete wave in a weakly radiating gas is thus apparent. At small times ($\tau < \sqrt{\gamma_0}$) the radiation from the wall builds up a compression-expansion wave, with magnitude of order $1/Bo_N$, over a distance of two or three radiative mean free paths from the wall. This small disturbance grows in magnitude with time, and its front begins to propagate

acoustically away from the wall. As time becomes of $O(\sqrt{\gamma_0})$ the resulting gas-dynamic wave front outruns the immediate effects of the wall radiation and travels as a discrete modified-classical wave at the isentropic speed of sound. The radiant energy input from the wall continues to increase the temperature and decrease the density over a distance of a few radiative mean free paths. By creating in this way an effective gas piston, it also produces the driving force that sustains the modified-classical wave at a constant magnitude during the intermediate-time region $\sqrt{\gamma_0} < \tau < Bo_N/16$. At large times ($\tau > Bo_N/16$) the radiative heat addition near the wall becomes essentially a diffusive process

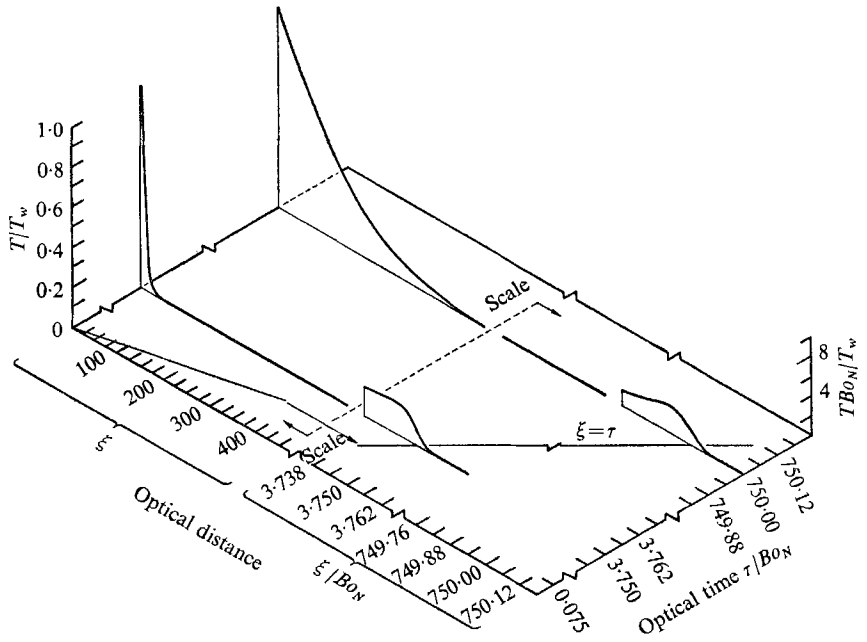

FIGURE 12. Temperature response for large time, $\gamma_0 = 1{\cdot}4$, $Bo_N = 2 \times 10^3$.

in an optically thick region. This process causes an increase in temperature and a decrease in density, with relatively negligible disturbances in velocity and pressure. Far ahead of this radiation-controlled region is a modified-classical wave front with small disturbances in all dependent variables. This wave front now decreases in strength and diffuses as a result of radiant heat transfer to its relatively cool surroundings and of the decreasing speed of the effective gas piston. As $\tau \to \infty$ the velocity and the pressure disturbance go everywhere to zero, and the final state of the gas is one of a uniform increase in temperature and corresponding decrease in density.

4. Solution for $Bo_N = O(16\sqrt{\gamma_0})$ and $Bo_N \ll 16\sqrt{\gamma_0}$

Here we outline the solution for $Bo_N = O(16\sqrt{\gamma_0})$ and $Bo_N \ll 16\sqrt{\gamma_0}$ without presenting the mathematics or giving plots of all the wave forms. Such treatment is possible because the basic phenomenology of the previous solution continues to hold for all Bo_N. The details do vary somewhat, but the general structure can

be understood with the aid of figure 1. The complete mathematical and graphical results are given by Cogley (1968). The case of $Bo_N = O(16\sqrt{\gamma_0})$ is discussed here, contrary to the procedure for the mechanically driven wave in Cogley & Vincenti (1969), because more detail is needed to understand the present, more complex problem. It will be evident as the discussion proceeds how the three cases fit together to provide an understanding of the solution for a continuous spectrum of Bo_N.

$$Bo_N = O(16\sqrt{\gamma_0})$$

To obtain the solution corresponding to small time in this case, c_S, c_∞ and the C's are expanded for $|s| > 16/Bo_N$. The resulting expressions are then used to find the dependent variables in the manner discussed in §3. The inversions for this time region can be found from tables. The solution that results is made up of a power series in τ identical to that given for $Bo_N \gg 16\sqrt{\gamma_0}$ by (2)–(5) and a now equally important power series in $16\tau/Bo_N$, which was negligible when $Bo_N \gg 16\sqrt{\gamma_0}$. This difference is reflected in figure 1, where the present small-time solution is bounded from above simultaneously by $16\tau/Bo_N = O(1)$ and $\tau = O(\sqrt{\gamma_0})$.

The large-time solution is found by expanding c_S, c_0 and the C's for $|s| < 16/Bo_N$. There is no intermediate-time region for this case, because of the mathematical structure of the c's and their regions of validity. This is evident in figure 1, where the intermediate-time regions for both large and small Bo_N are shown to degenerate into merely a transition region as Bo_N approaches $O(16\sqrt{\gamma_0})$ from either side. The inversion in the large-time region employs the techniques of steepest descent and convolution, and the function representing the speed of the effective gas piston, which drives the modified-classical velocity contribution, is handled in a manner similar to that for the large-time solution in §3. The resulting solution is identical in its lowest-order terms to the large-time solution for $Bo_N \gg 16\sqrt{\gamma_0}$ (cf. (25)–(27)).

We now see how the solution must evolve as Bo_N goes from $O(16\sqrt{\gamma_0})$ to larger values. The two small-time solutions differ by the presence of a power series in $16\tau/Bo_N$ for $Bo_N = O(16\sqrt{\gamma_0})$. Since this series is negligible for larger Bo_N, the power series in τ becomes dominant, which causes the region of validity to be bounded from above by $\tau = O(\sqrt{\gamma_0})$ (cf. figure 1). The two large-time solutions are identical to first order, with the additional higher-order terms present for $Bo_N = O(16\sqrt{\gamma_0})$ becoming negligible as Bo_N increases. In both large-time solutions the region of validity is given by $16\tau/Bo_N > 1$. The growing range of τ between the small- and large-time regions (cf. figure 1) is filled in by the intermediate-time solution of §3.

As before, the radiative heat addition gives rise at small time to a compression-expansion wave with a wave front that is radiation controlled. The perturbations in all dependent variables are larger than those for $Bo_N \gg 16\sqrt{\gamma_0}$, since the level of radiant transfer is now larger. The wave forms, however, are generally similar to those given in figures 2–4. The temperature discontinuity at the wall has the same characteristic decay time of $\tau = Bo_N/16$. As a result, it now essentially disappears by the end of the present small-time region.

At large time the solution again shows the continuation of the characteristic compression-expansion wave built up at small times. Within the transition region at $16\tau/Bo_N = O(1)$, the radiation-controlled wave front from small times has outrun the wall radiation and is now propagating away from the wall as a modified-classical wave at the isentropic speed of sound. The radiation from the wall continues to cause an expansion of the gas optically close to the wall. As in §3, the velocity of the resulting gas piston decreases at large time like $1/\sqrt{\tau}$. The modified-classical wave driven by the piston again decreases in magnitude like $1/\sqrt{\tau}$ and spreads out like $\sqrt{\tau}$. These phenomena are apparent in plots of the large-time density and temperature for $Bo_N = 10$ in figures 13 and 14. The

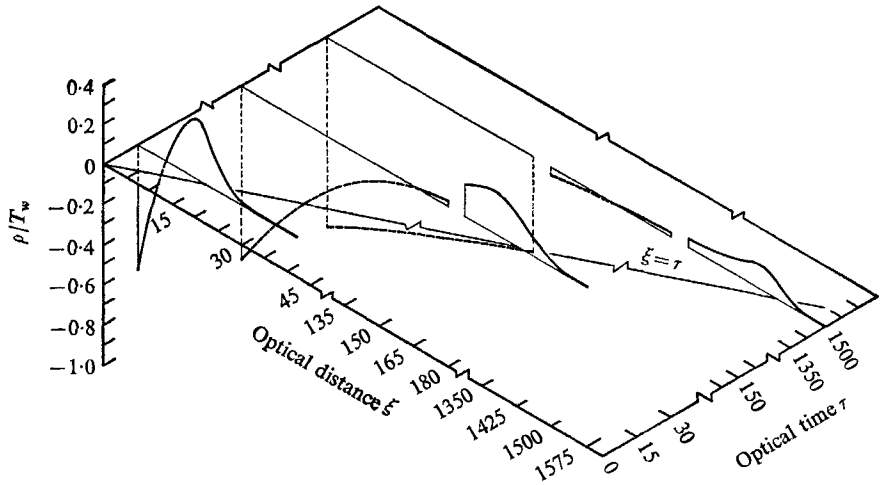

FIGURE 13. Density response for large time, $\gamma_0 = 1{\cdot}4$, $Bo_N = 10$.

density plot shows the compression-expansion wave with the modified-classical wave front decreasing in magnitude and diffusing as it propagates. The perturbation in density optically close to the wall, where the gas receives radiant energy directly from the wall, is much larger than that at the wave front. The same is true for the temperature, whose wave form is particularly interesting in that it shows the modified-classical wave just emerging from the radiation-controlled effects at the smallest time ($\tau = 15$). In both plots the modified-classical part of the wave propagates into the gas along $\xi = \tau$, while the radiation-controlled part diffuses into the gas like erfc $[\frac{1}{2}\xi(Bo_N/16\tau)^{\frac{1}{2}}]$.

$$Bo_N \ll 16\sqrt{\gamma_0} \quad (\textit{strong radiation})$$

The basic approach here parallels that of the preceding cases, and the basic phenomenology is much the same. Its occurrence in the ξ, τ plane, however, is different, and it is this difference that we wish to emphasize.

The small-time solution is obtained by expanding c_S, c_∞ and the C's for $|s| > 16/Bo_N$ (see (1.33, 1.35) and (1.30, 1.31), respectively). The resulting expressions are then used, as before, to obtain a solution that is identical to the one found for small time when $Bo_N = O(16\sqrt{\gamma_0})$, except that we drop the now negligible power

series in τ. This solution has a region of validity bounded from above by the transition region $16\tau/Bo_N = O(1)$, as shown in figure 1. When Bo_N is small, the solution is valid only for very small values of τ, and its region of validity vanishes as $Bo_N \to 0$.

The small-time solution gives rise once again to a compression-expansion wave, with the wave front controlled by radiation. Because of increased radiative transfer and the small time for which the present solution is valid, the radiation-controlled wave front is now felt very far ahead of the modified-classical contribution. The high level of radiative transfer also causes the perturbations in the

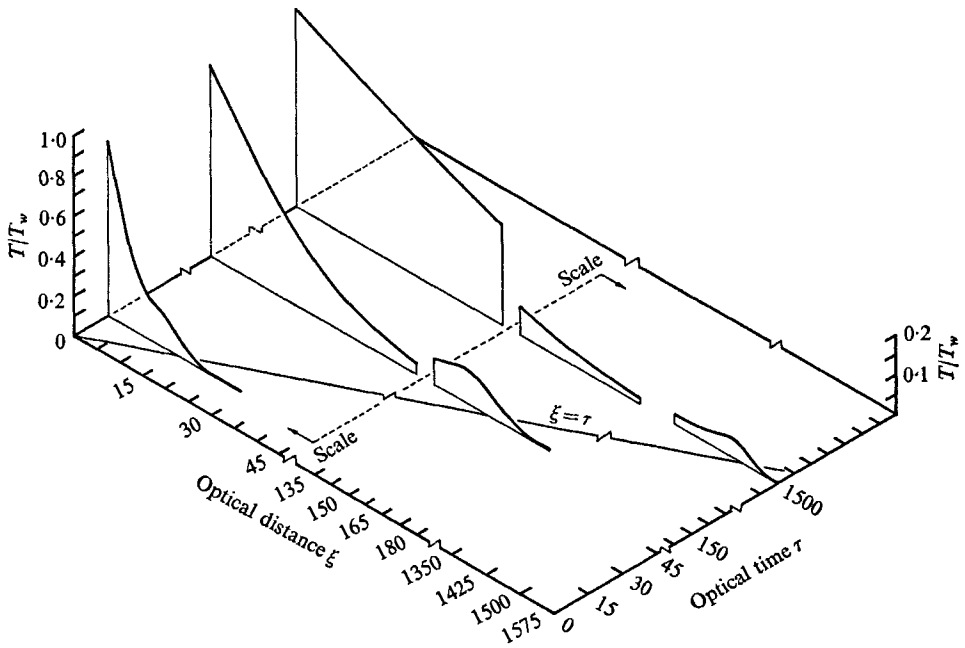

FIGURE 14. Temperature response for large time, $\gamma_0 = 1{\cdot}4$, $Bo_N = 10$.

dependent variables to be larger than in the earlier cases. For this reason the temperature discontinuity at the wall decays rapidly in this time region and essentially disappears as $\tau \to O(Bo_N/16)$. This same dimensionless time for decay was observed for all other values of Bo_N and represents an overall parameter for decay as indicated in figure 1.

An intermediate-time solution appears again at small Boltzmann numbers. This is dictated by the results of the harmonic solution discussed in Cogley & Vincenti (1969, §4), which are reflected in the mathematical expressions of the approximate c's. It is in this region that the isothermal solution (1.34) plays a role. The quantities c_T, c_∞ and the C's are expanded in the annular region $Bo_N/16\gamma_0 < |s| < 16/Bo_N$ to find the needed expressions for use in the solution equation (1.37). The solution is inverted by means of convolution, steepest descent and tables and is valid in the region $Bo_N/16 < \tau < 16\gamma_0/Bo_N$.

The intermediate-time solution shows that the radiative heat addition is now

a diffusive process. (The transition to this type of radiative transport takes place generally for all Bo_N across the transition region denoted by $16\tau/Bo_N = O(1)$ in figure 1.) That is to say, the gas has been sufficiently heated that the gaseous radiation due to spontaneous emission is as important as the radiation from the wall. The solution also exhibits the continuation of the compression-expansion wave built up at small times. In contrast to the intermediate-time solution for $Bo_N \gg 16\sqrt{\gamma_0}$, however, the compressive wave front is now still radiation-controlled and is characterized by complementary-error-function terms from the radiation-controlled contribution. This wave front is followed by a modified-classical expansion wave that propagates into the gas at the isothermal speed of sound and acts as a boundary layer to the radiation-controlled contribution.

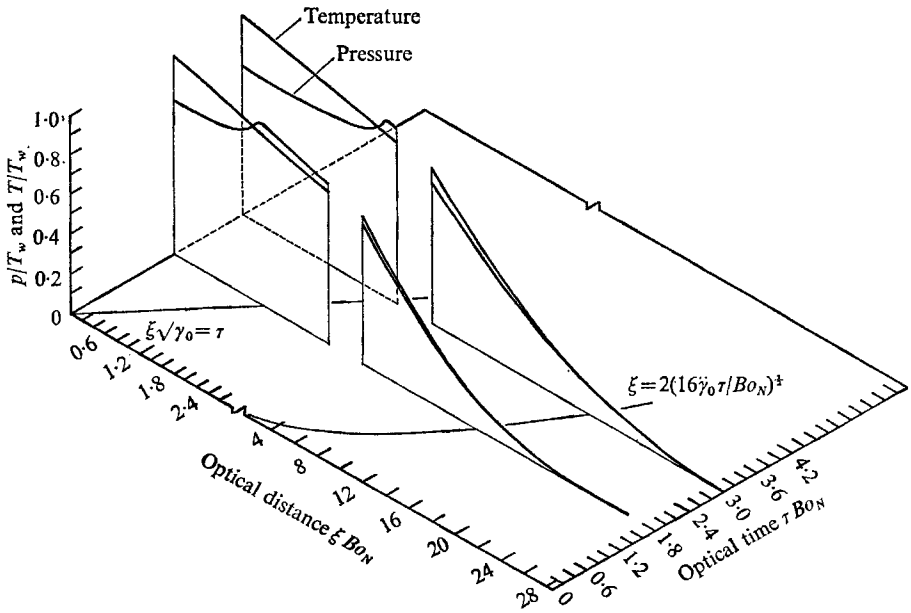

FIGURE 15. Temperature and pressure response for intermediate time, $\gamma_0 = 1{\cdot}4$, $Bo_N = 2 \times 10^{-3}$.

These details are illustrated in figure 15 in a combined plot of temperature and pressure for $Bo_N = 2 \times 10^{-3}$ in the intermediate-time region. The radiation-controlled wave front diffuses into the gas like $\operatorname{erfc}[(\xi/2)(Bo_N/16\gamma_0\tau)^{\frac{1}{2}}]$ and thus decays about the parabolic line $\xi = 2(16\gamma_0\tau/Bo_N)^{\frac{1}{2}}$. The decrease in pressure at $\xi < \tau/\sqrt{\gamma_0}$ is due to the modified-classical expansion wave. This wave travels at the isothermal speed of sound, since it propagates in a strong radiative field that maintains an essentially constant temperature through the wave. It has effects to a depth slightly beyond $\xi = \tau/\sqrt{\gamma_0}$ as a result of diffusion.

The wave forms in figure 15 are in many respects similar to those presented in figure 4 for the small-time solutions when $Bo_N \gg 16\sqrt{\gamma_0}$. This similarity is tied in with the change that takes place in the transition region defined by $Bo_N\tau/16\gamma_0 = O(1)$ and $\tau = O(\sqrt{\gamma_0})$ in figure 1. In passing through this region from smaller to larger τ, the wave front changes from radiation-controlled to modified-classical,

as observed in the solutions for the two earlier cases. All solutions for τ prior to this region have essentially similar flow fields, by virtue of their relation to the transition. We can therefore expect that once the straight and parabolic paths in figure 15 intersect at larger time, the present radiation-controlled wave front will be replaced by a modified-classical front propagating at the isentropic speed of sound. We anticipate the isentropic speed since the wave front should then be optically so thick that radiative transfer within it is negligible.

From figure 1 we see that the intermediate-time solution becomes the entire solution as $Bo_N \to 0$. In this limit the solution reduces to

$$\left.\frac{u}{T_w}\right|_{Bo_N\to 0} = \left.\frac{\rho}{T_w}\right|_{Bo_N\to 0} \to 0,$$

$$\left.\frac{p}{T_w}\right|_{Bo_N\to 0} = \left.\frac{T}{T_w}\right|_{Bo_N\to 0} \to 1$$

(cf. Cogley 1968).This is the same result that one would obtain by first taking the limit $Bo_N \to 0$ of the exact governing equation (1.6) and then solving the present problem. This limiting solution represents an instantaneous uniform heating of the entire expanse of gas to the temperature of the wall, with a corresponding increase in pressure. This is a reasonable result, since the radiative heat transfer becomes infinite as $Bo_N \to 0$.

The solution for large time is found by expanding c_S, c_0 and the C's for $|s| < Bo_N/16\gamma_0$. The general method is again similar to that for large time in the earlier cases. The details, however, are more involved; anyone setting out to carry them though may wish to consult Cogley (1968).

That the expectations discussed above are correct is shown in figure 16, where the velocity and pressure for $Bo_N = 2 \times 10^{-3}$ are plotted for two representative large times. The characteristic straight and parabolic lines are seen here to have crossed. The difference by the factor γ_0 in the parabolic paths for the intermediate- and large-time regions reflects the difference between the infinite- and zero-speed equations used in the solution. The modified-classical contribution now forms the compressive wave front; the radiation-controlled contribution has become the expansion region, which now acts as a boundary layer to the modified-classical wave. The corresponding plots for temperature and density (see Cogley 1968) are qualitatively similar to those of figures 11 and 12 for the large-time solution when $Bo_N \gg 16\sqrt{\gamma_0}$. Note also the qualitative resemblance of figure 16 to figure 10.

The overall phenomenology for $Bo_N \ll 16\sqrt{\gamma_0}$ (strong radiation) is clear. At small times ($\tau < Bo_N/16$) the radiant heat addition gives rise once more to a compression–expansion wave in the gas. Because of the rapid heating, the radiative heat addition now becomes a diffusive process at the relatively early time $\tau = O(Bo_N/16)$. At intermediate times ($Bo_N/16 < \tau < 16\gamma_0/Bo_N$), the radiative heat addition from the wall continues to control the now diffusive wave front, which is located around $\xi = 2(16\gamma_0\tau/Bo_N)^{\frac{1}{2}}$. The compression-expansion wave continues its development, with the expansion part of the wave being given by an isothermal modified-classical contribution. The gas-dynamic disturbance now outruns the immediate effects of the wall radiation

only at the end of the intermediate-time region, and only then does the wave front begin to propagate as a modified-classical wave. At large times this wave front propagates into the gas at the isentropic speed of sound. As for weak radiation, the heat addition from the wall drives the modified-classical wave indirectly, by forming an effective gas piston whose speed decreases in

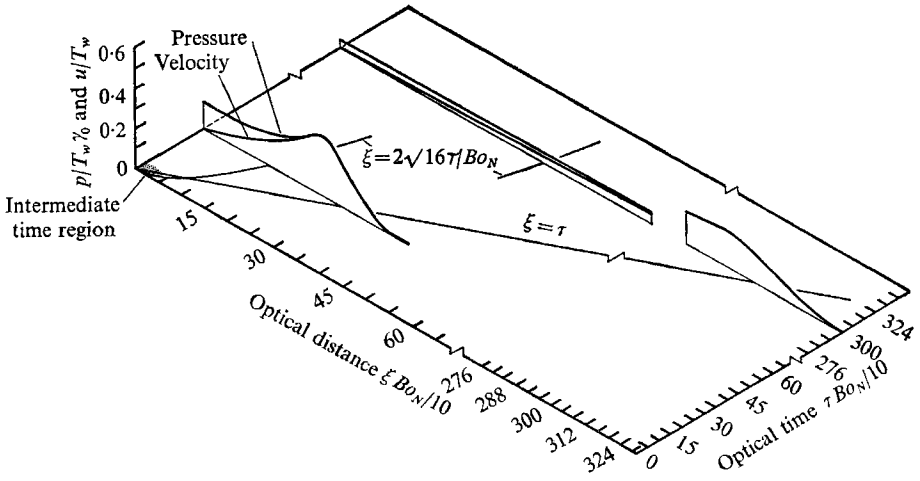

FIGURE 16. Velocity and pressure response for large time, $\gamma_0 = 1{\cdot}4$, $Bo_N = 2 \times 10^{-3}$.

this region like $1/\sqrt{\tau}$. This portion of the total wave again decays and diffuses as it travels. The radiation-controlled contribution causes an increase in temperature and a decrease in density in a growing region next to the wall, and the final state of the gas as $\tau \to \infty$ and the wave front moves to infinity is again given by u/T_w and $p/T_w \to 0$, $T/T_w \to 1$, and $\rho/T_w \to -1$.

5. Limited solution for $16\tau/Bo_N < 1$

If one examines all the foregoing solutions that are valid for $16\tau/Bo_N < 1$ (see figure 1), a common characteristic is evident. In all instances the net radiative heat addition is by simple absorption from the wall, to the order of terms retained (see figure 1). This can be seen explicitly by calculating the negative gradient (i.e. the negative divergence) of the radiative heat flux $\hat{q}^R$ for these solutions. The gradient of the heat flux is related to the potential function and thence to the physical quantities by

$$\frac{\partial \hat{q}^R}{\partial \xi} = \frac{\partial^2 \phi}{\partial \tau^2} - \frac{\partial^2 \phi}{\partial \xi^2} = -\frac{1}{\gamma_0}\frac{\partial p}{\partial \tau} + \frac{\partial \rho}{\partial \tau},$$

(see material preceding (1.7)). Using this equation one can evaluate $-\partial \hat{q}^R/\partial \xi$, in particular, for all the solutions valid for $16\tau/Bo_N < 1$. (Those written down in this paper are given by (2)–(5) and (12)–(15).) The result is

$$-\frac{\partial \hat{q}^R}{\partial \xi} = \frac{8T_w}{Bo_N} e^{-\xi} + O\left(\frac{\tau 16^2 T_w}{2Bo_N^2} e^{-\xi}\right), \tag{28}$$

where $T_w = 0$ for $\tau \leqslant 0$.

We can use this result to derive an approximate acoustic equation valid for all Bo_N and for τ such that the restriction $16\tau/Bo_N < 1$ holds. To this end we incorporate this first term on the right-hand side of (28) into the linearlized one-dimensional gas-dynamic equations (cf. Gilles *et al.* 1969) to obtain:

$$\frac{\partial \rho}{\partial \tau} + \frac{\partial u}{\partial \xi} = 0,$$

$$\gamma_0 \frac{\partial u}{\partial \tau} + \frac{\partial p}{\partial \xi} = 0,$$

$$\frac{\partial h}{\partial \tau} + \frac{(\gamma_0 - 1)}{\gamma_0} \frac{\partial p}{\partial \tau} = -\frac{\partial \hat{q}^R}{\partial \xi} = \frac{8T_w}{Bo_N} e^{-\xi},$$

$$h = p - \rho.$$

Elimination between these equations gives the following inhomogeneous wave equation for velocity

$$\frac{\partial^2 u}{\partial \xi^2} - \frac{\partial^2 u}{\partial \tau^2} = \begin{cases} 0 & (\tau \leqslant 0), \\ -\dfrac{8T_w}{Bo_N} e^{-\xi} & (\tau > 0). \end{cases} \tag{29}$$

The initial and boundary conditions for the present problem are:

$$\tau = 0, \quad \xi \geqslant 0; \quad u = 0, \quad \frac{\partial u}{\partial \tau} = 0,$$

$$\tau > 0, \quad \xi = 0; \quad u = 0,$$

$$\tau > 0, \quad \xi \to \infty; \quad u \to 0.$$

The foregoing problem can be solved by the use of Riemann's function; this standard method is outlined in, e.g. Courant & Hilbert (1962). The solution can be written down at once as

$$\frac{uBo_N}{T_w} = \begin{cases} 4\{\exp[-(\xi+\tau)] + \exp[-(\xi-\tau)] - 2\exp(-\xi)\} & (\xi-\tau > 0), \\ 4\{2 - \exp[-(\tau-\xi)] - 2\exp(-\xi) + \exp[-(\xi+\tau)]\} & (\xi-\tau < 0). \end{cases} \tag{30}$$

The equations of conservation of mass and momentum plus the state equation lead to the following solution for the other dependent variables:

$$\frac{pBo_N}{T_w} = \begin{cases} 4\gamma_0\{\exp[-(\xi-\tau)] - \exp[-(\xi+\tau)]\} & (\xi-\tau > 0), \\ 4\gamma_0\{2 - \exp[-(\tau-\xi)] - \exp[-(\xi+\tau)]\} & (\xi-\tau < 0), \end{cases} \tag{31}$$

$$\frac{\rho Bo_N}{T_w} = \begin{cases} -4\{2\tau\exp(-\xi) + \exp[-(\xi+\tau)] + \exp[-(\xi-\tau)]\} & (\xi-\tau > 0), \\ -4\{2\tau\exp(-\xi) + \exp[-(\xi+\tau)] + \exp[-(\tau-\xi)] - 2\} & (\xi-\tau < 0), \end{cases}$$

$$\frac{TBo_N}{T_w} \tag{32}$$

$$= \begin{cases} 4\{2\tau\exp(-\xi) + (\gamma_0 - 1)[\exp[-(\xi-\tau)] - \exp[-(\xi+\tau)]]\} & (\xi-\tau > 0), \\ 4\{2\tau\exp(-\xi) + (\gamma_0 - 1)[2 - \exp[-(\tau-\xi)] - \exp[-(\xi+\tau)]]\} & (\xi-\tau < 0). \end{cases} \tag{33}$$

This solution is valid for all Bo_N and τ such that $16\tau/Bo_N < 1$. As discussed in §3, the solution agrees within a few per cent with those found earlier except at the wave front in the intermediate-time solution for $Bo_N \gg 16\sqrt{\gamma_0}$ (see figure 6). The reason for this was explained in §3, and the present solution was used to provide a more accurate wave front in the plotted results for that section.

The fact that the gradient of the heat flux decays like $\exp(-\xi)$ when $16\tau/Bo_N < 1$ (the pure exponential is due to the substitute-kernel approximation) means that the gas in this situation acts as a simple absorber, i.e. the radiative heat addition is due to emission from the wall only. We may therefore call this region of the Bo_N, τ plane of figure 1 'absorption dominated'. A more complete explanation and exploitation of the special properties of this region will be made in a later paper.

6. Concluding remarks

The questions one must ask of any new approximate solution to a physical problem as complex as this are: (i) Does it tell a physically plausible and consistent story? (ii) Does it agree with what is already known from work on related problems? The answer to the first question is yes, since the results of the preceding sections do hang together in a physically sensible way. The second question can be answered by examining the relationship of the present solution to the limited work done on similar problems.

As mentioned in §1, Baldwin (1962) has discussed the present problem in a limited way by an entirely different method. In appendix H of his paper, he gave an approximate solution for the temperature wave form that is 'correct for all limiting values of the variables and parameters'. A comparison with the present solution shows that his approach omits the important modified-classical contribution retained in the present analysis. Insofar as the radiation-controlled contribution alone is concerned, however, his temperature results do agree identically with ours when specialized to our time regions. Baldwin also gave a qualitative discussion of the velocity wave form, and this discussion can be correlated with the present solution.

Solan & Cohen (1966) also presented a limited solution related to the present work. Their solution, as discussed in §1, is analogous to that carried out in §5 and is limited essentially by the restriction (in present notation) that $16\tau/Bo_N < 1$. Solan & Cohen's work was for a grey gas and retained the non-linear boundary condition at the wall. Their plotted results, however, are qualitatively similar to those given here in figures 2–4. Results corresponding to our figures 7–9 were not presented.

An interesting comparison can also be made between the present results and the nuclear-fireball phenomenology discussed by Brode (1964). The early stages in the fireball (i.e. for very short times after detonation) are the non-linear counterpart of the present problem, in that radiation from an essentially constant-temperature source plays the major role in setting up the wave phenomena. If we keep in mind the well-known differences between linear and non-linear wave problems, the similarity of the response in the two problems is striking.

According to Brode, the radiation from the nuclear explosion initially causes a very steep radiation-controlled wave front. This is the non-linear counterpart of the smooth radiation-controlled wave front of the present problem, the steepness of the wave front in the explosion being caused by the non-linear effect of the varying absorption coefficient. The density increases only slightly near the non-linear radiation-controlled front and then decreases behind it to form a compression-expansion wave equivalent to that found here. As time increases (although still remaining very small), the steep disturbance caused by the radiant heat addition outruns the immediate effects of the radiation and begins to form a classical adiabatic shock wave. This process is the non-linear counterpart to the present transition from the smooth radiation-controlled wave front to the diffuse modified-classical front. The non-linear problem also exhibits the typical overpressures that are observed in figure 15 just before the transition takes place. The analogy breaks down after the initial stages of the fireball because the case shock, caused by the mechanical explosion itself, comes into play.

Our entire study rests, of course, on the use of the exponential approximation for the transmission functions that appear in the equations for the non-grey radiative flux (cf. Gilles *et al.* 1969). This is a non-rational approximation, and its accuracy is difficult to evaluate without extensive numerical calculations. A number of investigations have shown, however, that the exponential approximation is certainly qualitatively valid. A limited solution to the present problem, independent of the exponential approximation, has been found, however (cf. Cogley 1968). This solution will be included in the paper mentioned at the end of §5.

Linearization has also been used throughout, and this can lead to inaccuracies at large time because of well-known, cumulative non-linear effects. Since the velocity disturbance is small and goes to zero for $\xi \to \infty$ in the present problem, these effects will be negligible for larger disturbances in the case under discussion than they would be in the case of the impulsively moving wall; i.e. the present solution is uniformly valid in the limit of a vanishingly small disturbance.

The author acknowledges a debt to Prof. Walter G. Vincenti for encouragement and advice throughout the research. Thanks are also extended to Walter A. Reinhardt of Ames Research Center and to Prof. Sau-Hai Lam of Princeton University. The work was supported by the U.S. Air Force Office of Scientific Research, contract AF 49(638)-1280. During part of the study, the author received a National Aeronautics and Space Administration Training Grant.

REFERENCES

BALDWIN, B. S. 1962 The propagation of plane acoustic waves in a radiating gas. *NASA* TR R-138.

BRODE, H. L. 1964 Fireball phenomenology. *RAND Corp.*, Report P-3026.

COGLEY, A. C. 1968 An approximate method for analyzing non-equilibrium acoustic phenomena with application to discrete radiation-driven waves. Ph.D. Thesis, Dept. of Aero. and Astro., Stanford University.

COGLEY, A. C. & VINCENTI, W. G. 1969 Application to radiative acoustics of Whitham's method for the analysis of non-equilibrium wave phenomena. *J. Fluid Mech.* **39**, 641.

COURANT, R. & HILBERT, D. 1962 *Methods of Mathematical Physics.* II. New York: Interscience.

ERDÉLYI, A. *et al.* 1954 *Tables of Integral Transforms.* New York: McGraw Hill.

GILLES, S. E., COGLEY, A. C. & VINCENTI, W. G. 1969 A substitute-kernel approximation for radiative transfer in a non-grey gas near equilibrium, with application to radiative acoustics. *Int. J. Heat and Mass Transfer*, **12**, 445.

LONG, H. R. & VINCENTI, W. G. 1967 Radiation-driven acoustic waves in a confined gas. *Phys. Fluids*, **10**, 1365.

SOLAN, A. & COHEN, I. M. 1966 Weakly radiative acoustic flow induced by radiation from a stationary wall. *Phys. Fluids*, **9**, 2365.

SOLAN, A. & COHEN, I. M. 1967*a* Rayleigh problem in a radiating compressible gas. Part 1. Plate mach number finite. *Phys. Fluids*, **10**, 108.

SOLAN, A. & COHEN, I. M. 1967*b* Rayleigh problem in a radiating compressible gas. Part 2. Plate mach number large. *Phys. Fluids*, **10**, 257.

WHITHAM, G. B. 1959 Some comments on wave propagation and shock wave structure with application to magnetohydrodynamics. *Comm. Pure Appl. Math.* **12**, 113.